Rhenium in Homogeneous Catalysis: [ReBrH(NO)(labile ligand) (large-bite-angle diphosphine)] Complexes as Highly Active Catalysts in Olefin Hydrogenations

ARTICLE *in* JOURNAL OF THE AMERICAN CHEMICAL SOCIETY · JUNE 2011

Impact Factor: 12.11 · DOI: 10.1021/ja107245k · Source: PubMed

4 AUTHORS, INCLUDING:

Kunjanpillai Rajesh
University of Zurich
7 PUBLICATIONS **86** CITATIONS
SEE PROFILE

Olivier Blacque
University of Zurich
186 PUBLICATIONS **2,369** CITATIONS
SEE PROFILE

Heinz Berke
University of Zurich
336 PUBLICATIONS **5,665** CITATIONS
SEE PROFILE

JACS
JOURNAL OF THE AMERICAN CHEMICAL SOCIETY

ARTICLE

pubs.acs.org/JACS

Rhenium in Homogeneous Catalysis: [ReBrH(NO)(labile ligand)(large-bite-angle diphosphine)] Complexes as Highly Active Catalysts in Olefin Hydrogenations

Balz Dudle, Kunjanpillai Rajesh, Olivier Blacque, and Heinz Berke*

Institute of Inorganic Chemistry, University of Zürich, Winterthurerstrasse 190, CH-8057 Zürich

Supporting Information

ABSTRACT: The reaction of [$ReBr_2$(MeCN)(NO)(P∩P)] (P∩P = 1,1′-bisdiphenylphosphinoferrocene (dppfc) (**1a**), 1,1′-bisdiisopropylphosphinopherrocene (diprpfc) (**1b**), 2,2′-bis(diphenylphosphino)diphenyl ether (dpephos) (**1c**), 10,11-dihydro-4,5-bis(diphenylphosphino)dibenzo[*b*,*f*]oxepine (homoxantphos) (**1d**) and 4,6-bis-(diphenylphosphino)-10,10-dimethylphenoxasilin (Sixantphos) (**1e**)) led in the presence of $HSiEt_3$ and ethylene to formation of the ethylene hydride complexes [ReBrH(η^2-C_2H_4)(NO)(P∩P)] (**3a**,**b**,**d**), the MeCN ethyl complex [ReBr(Et)(MeCN)(NO)(dpephos)] (**5c**) and two ortho-metalated stereoisomers of [ReBr(η^2-C_2H_4)(NO)(η^3-*o*-C_6H_4−Sixantphos)] **8e(up)** and **8e(down)**. The complexes **3a**,**b**,**d**, and **5c** and the isomers of **8e** showed high catalytic activity (TOFs ranging from 22 to 4870 h^{-1}, TONs up to 24000) in the hydrogenation of monosubstituted olefins. For **8e(down)** and **8e(up)** a remarkable functional group tolerance and catalyst stability were noticed. Kinetic experiments revealed k_{obs} to be first order in c(cat) and c(H_2) and zeroth order in c(olefin). Mechanistic studies and DFT calculations suggest the catalysis to proceed along an Osborn-type catalytic cycle with olefin before H_2 addition. The unsaturated key intermediates [ReBrH(NO)(P∩P)] (**2a**−**e**) could be intercepted with MeCN as [ReBrH(MeCN)(NO)(P∩P)] (**10a**−**d**) complexes or isolated as dimeric μ^2-$(H)_2$ complexes [{ReBr(μ^2-H)(NO)(P∩P)}$_2$] (**9b** and **9e**). Variation of the bidentate ligand demonstrated a crucial influence of the (large)-bite-angle on the catalytic performance and reactivity of **3a**,**b**,**d**, **5c**, and **8e**.

1. INTRODUCTION

Catalytic Wilkinson and Osborn-type hydrogenations of unsaturated organic compounds are widely applied. Their mechanisms were studied in detail and are well understood.[1] Highly active and selective catalysts are available to hydrogenate various unsaturated substrates and make it a method of choice for environmentally benign and enantioselective reductions.[2] Although the field of catalytic hydrogenations seems to be quite mature, fundamental challenges remained. The fact that most of the homogeneous hydrogenations require platinum group metal centers may cause future resource problems and makes it necessary to fully recycle the catalyst in industrial processes. In addition, because of toxicity reasons,[3] pharmaceutical products produced by such catalyzes have to be freed from the precious metals to the ppm level.[4] Often precious metal catalysis also suffers from reduction to the metals under hydrogenation conditions[5] resulting in loss of activity and/or selectivity. These latter disadvantages were anticipated to be circumvented by the use of transition metal catalysts less "noble" in character. The element rhenium being border to the precious metals has preserved at least some of the precious metal's character, as for instance the preference for interaction with H_2[6] and olefins.[7] These chemical properties made us believe that appropriate rhenium complexes could be efficient hydrogenation catalysts. We therefore targeted the development of new rhenium nitrosyl complexes also on the basis of their isoelectronic relationship to ruthenium carbonyl or phosphine or rhodium halide fragments, which comprise essential building blocks of effective hydrogenation[8] and hydroformylation[9] catalysts.

Our research group has accumulated considerable experience in the realm of rhenium nitrosyl chemistry, and we could recently demonstrated that *trans*-[ReH_2(η^2-C_2H_4)(NO)(PR_3)$_2$] (R = *i*pr, cy) complexes catalyze the hydrogenation of simple olefins and ketones,[10] as well as hydrogen-related reactions, such as hydrosilylations, dehydrogenative silylations,[11] and dehydrogenative aminoborane coupling reactions.[12] We expected improvement of the catalytic performance of these complexes by forcing the phosphines into cis positions by applying chelate diphosphines. Therefore, we approached the preparation of rhenium complexes of the type [ReHBrL(NO)(P∩P)] with L, representing a labile ligand, and P∩P, a large-bite-angle chelate diphosphine, and their use as precatalysts in olefin hydrogenations.

2. RESULTS AND DISCUSSION

2.1. Preparation of Ethylene Hydride Complexes 3a−d. From our work on the bromide complexes [$ReBr_2$(MeCN)(NO)(P∩P)]

Received: August 23, 2010
Published: April 25, 2011

(P∩P = dppfc (**1a**), diprpfc (**1b**), dpephos (**1c**), homoxantphos (**1d**), or Sixantphos (**1e**))[13] we learned that the unsupported 16e$^-$ species [ReBrH(NO)(P∩P)] (**2a**−**e**) are unstable, hence not suited as catalyst precursors and needed to be generated in situ for catalytic applications. We reckoned that these unsaturated complexes could be reversibly generated from [$ReBrH_2(SiEt_3)$(NO)(P∩P)] in the presence of $HSiEt_3$. However, with the exception of the diprpfc derivative, these complexes were still too reactive to be employed as isolable precatalysts.[13] Therefore, we attempted the reaction of **1a**−**e** with $HSiEt_3$ in the presence of ethylene as an additional auxiliary (Scheme 1). Ethylene was considered an ideal ligand for the stabilization of the 16e$^-$ species **2a**−**e**, because of its small size and appropriate binding capabilities to electron-rich Re(I) centers.[7,10] Additionally, in view of the application of the expected [ReBrH(η^2-C_2H_4)(NO)(P∩P)] (**3a**−**e**) compounds to function as a precatalyst in hydrogenation catalyzes, the ethylene ligand was anticipated to be initially hydrogenated to ethane, releasing the desired highly reactive **2a**−**e** intermediates, which could then drive the catalytic cycle (Scheme 1).

The reactions of **1a**, **1b**, and **1d** with an excess of $HSiEt_3$ proceeded smoothly in the presence of 2 bar of ethylene forming the isolable [ReBrH(η^2-C_2H_4)(NO)(P∩P)] complexes **3a**, **3b**, and **3d**. Monitoring the reactions by ^{31}P NMR showed almost quantitative conversions. The isolated yields were however somewhat lower (**3a**: 70%; **3b**: 61%; **3d**: 81%). On the basis of their spectroscopic features[14] **3a**, **b**, and **d** were assigned pseudo-octahedral structures with *trans*-Br and -NO ligands stabilized by a strong π push−pull interaction. The X-ray diffraction study of **3d** confirmed the proposed structure (Figure 1). It displayed NO/Br disorder, which indicated the presence of two isomeric forms of **3d** in the solid state. This isomerism turned out to be of negligible importance for the catalytic performance of these species (vide infra). The geometrical aspects of this isomerism are related to those of [$ReBr_2$(MeCN)(NO)(P∩P)] systems and were discussed in depth along with the stereochemistry of these complexes.[13]

Unlike in the cases of **1a**, **b**, and **d**, the reaction of **1c** with $HSiEt_3$ and ethylene did not afford the ethylene hydride complex **3c**, rather the MeCN ethyl derivative [ReBr(Et)(MeCN)(NO)-(dpephos)] (**5c**),[14] which could be rationalized on the basis of the initial formation of **3c**, which according to Scheme 1 undergoes a β-hydride shift to form the 16e$^-$ intermediate [ReBr(Et)(NO)(dpephos)] (**4c**). The stabilization arising from the addition of MeCN to **4c** forming **5c** is in the case of the dpephos derivative sufficiently high to shift the equilibrium of eq 1 quantitatively to the right side.

$$\mathbf{3c} + \mathrm{MeCN} \rightleftarrows \mathbf{5c} \qquad (1)$$

Reacting **1e** in the presence of ethylene with $HSiEt_3$ produced two ortho metalated isomers [$\overline{ReBr(\eta^2\text{-}C_2H_4)(NO)(\eta^3\text{-}C_6H_4\text{-}o\text{-Sixantphos})}$] **8e(up)** and **8e(down)**, which were characterized structurally.[14] Unlike in the previous cases, where an up/down isomerism was proposed on the basis of X-ray structures and $^{31}P\{^1H\}$ NMR spectra,[13,14] the **8(up/down)** isomers could be separated and were individually characterized. **8e(up/down)** proved to be kinetically stable in solution. We propose the ortho metalation to proceed via the unsaturated 16e$^-$ species [ReBrH(NO)(Sixantphos)] (**2e**). This species is not sufficiently stabilized by the binding of C_2H_4 or MeCN, but it is reactive enough to activate the *o*-C−H bond of one Sixanphos phenyl units forming the [$\overline{ReBr(H_2)(NO)(\eta^3\text{-}C_6H_4\text{-}o\text{-Sixantphos})}$] species (**6e**), which in turn can undergo a H_2/C_2H_4 ligand exchange via [$\overline{ReBr(NO)(\eta^3\text{-}C_6H_4\text{-}o\text{-Sixantphos})}$] (**7e**) resulting in the **8e(up/down)** isomers (Scheme 2).

2.2. Hydrogenation Using 3a,b,d, 5c, and 8e(up/down) as Catalysts. **3a,b,d**, **5c**, and **8e(up/down)** turned out to be (pre)catalysts for the hydrogenation of olefins comparable in activity to Wilkinson or Osborn-type Rh catalysts.[1,15] To explore

Scheme 1. Synthetic Access to and Reactivity of the Monohydride Species [ReHBr(NO)(P∩P)]

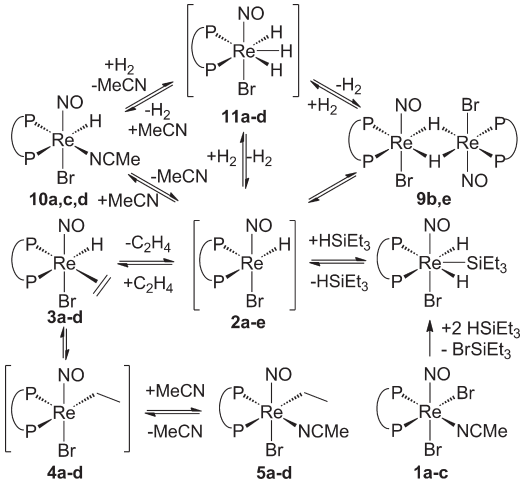

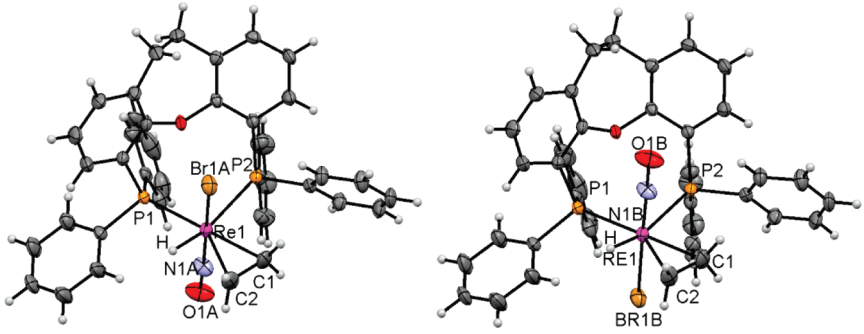

Figure 1. ORTEP diagram of **3d(down)** (left) is 85% populated, and **3d(up)** (right) is 15% populated drawn at 50% probability. Selected bond lengths [Å]: Br1A−Re1 2.5546(4), C1−C2 1.401(4), C1−Re1 2.242(3), C2−Re2 2.216(2), H−Re1 1.59, N1A−Re1 1.771(4), N1A−O1A 1.184(4), P1−Re1 2.4597(7), P2−Re1 2.5691(6). Selected bond angles [deg]: Br1A−Re1−N1A 175.5(4), Br1A−Re−Br1B 168.82(7), C1−Re−C2 36.63(10), C1−Re−P2 83.63(7), C2−Re−H 65, H−Re1−P1 80, P1−Re1−P2 95.22(2).

dx.doi.org/10.1021/ja107245k |*J. Am. Chem. Soc.* 2011, 133, 8168–8178

the catalytic capabilities of **3a**,**b**,**d**, **5c**, and **8e** in the catalytic hydrogenations of olefins, we employed a press gas flow controller for quantitative kinetic monitoring. The hydrogenations of 1-hexene and styrene were selected as benchmark processes to enable comparison in catalytic activities. Kinetic isotope effects were also probed for **3a**−**d** in the hydrogenations/deuterations of 1-hexene using the same set up. The found reaction rates are listed in the form of TOFs in Table 1 together with the conditions of the catalytic transformations.

The reaction rates were found to be zeroth order in c(olefin). This implies relatively strong olefin binding and a high olefin affinity of the rhenium center, which leads at already very low c(olefin) values to quantitative olefin saturation of the catalyst. Furthermore, the hydrogenation rate was found to be first order in p_{H_2}. This implies that H_2 saturation cannot be achieved under the employed conditions (Table 1). This behavior is often observed for hydrogenation catalysts.[1b] Moreover, probing the kinetic isotope effect (KIE) with D_2 revealed k_{D2} and k_{H2} to be practically identical (KIE = 1), which is not unusual for catalytic hydrogenation processes proceeding with homolytic splitting of H_2/D_2 (for the Wilkinson catalysts k_{H2}/k_{D2} was reported to be 0.9,[1] whereas for the Osborn catalyst it was reported to be 1.04[16]). From this result it seems improbable that a unique elementary step with prominent H/D participation, such as the oxidative addition of H_2 or D_2 or the reductive elimination of the product or the β-hydride shift, is uniquely rate limiting, since all these elementary-type reactions would be associated with a significantly higher KIE.[17] One aspect, which even further complicates the interpretation of the KIE, is the fact that the ethylene hydride complexes **3a**−**d** undergo fast reversible β-hydride shift reactions, and can therefore scramble the D(Re) content into the coordinated olefin (eq 2). In the case of **3a** (vide infra) this reaction is approximately 20 times faster than the hydrogenation of 1-hexene (Table 1).

Scheme 2. Transformation of 8e(up/down) into 3e(up/down)

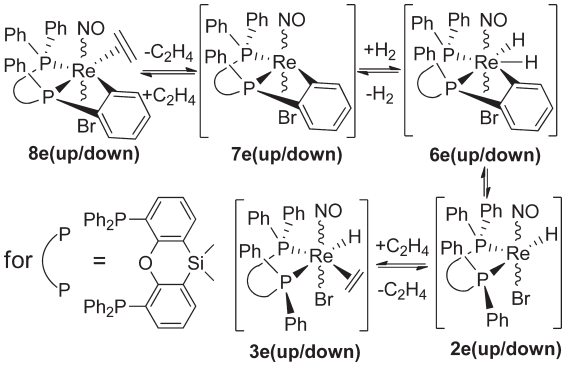

$$[\mathrm{ReBrD(H_2C{=}CHR)(NO)(P{\cap}P)}] \rightleftarrows [\mathrm{ReBrH(HDC{=}CHR)(NO)(P{\cap}P)}] \quad (2)$$

Since we could envisage that non-hydrogen-related steps, such as ligand exchanges, are also rate limiting or that KIE cancellations of hydrogen-related steps would occur, we cannot draw a clear overall picture of the components contributing to the KIE.

In the case of the hydrogenations of 1-hexene, very slow time-dependent decreases in activity were observed under the given conditions, indicating the catalytic systems to be fairly stable. In the case of **3a**,**b** and **5c**, replacement of THF with DCM led to a much faster decrease of the reaction rates, which was interpreted in terms of a progressing catalyst decomposition presumably via

Table 1. Catalytic Hydrogenation Using 3a,b,d, 5c, and 8e(up/down) as Catalysts

catalyst	loading (mol %)	substrate (mL)	solvent (mL)	temp. (°C)	p_{H_2} (bar)	TOF (h^{-1})	TON
3a	0.14	1-hexene (1)	THF (2)	23	10	290 [a]	700
3a	0.10	styrene (1)	THF (2)	23	10	386 [a]	900
3b	0.50	1-hexene (1)	toluene (8)	23	10	22 [b]	500
3b	0.42	1-hexene (2)	THF (10)	60	10	144 [a]	240
3b	0.42	1-hexene (2)	THF (10)	80	10	750 [a]	240
3c/5c	0.08	1-hexene (1)	THF (2)	23	10	1248 [a]	1200
3c/5c	0.09	styrene (1)	THF (2)	23	10	823 [a]	1000
3d [c]	0.06	1-hexene (1)	THF (2)	23	10	1050 [a]	1600
3d [c]	0.09	styrene (1)	THF (2)	23	10	1020 [a]	1100
8e(up) [d]	0.005	hexene (15)	toluene (10)	80	10	4120 [a]	5000
8e(up) [d]	0.004	styrene (15)	toluene (10)	80	10	2961 [a]	24100
8e(up) [d]	0.004	cyclohexene (15)	toluene (10)	120	10	1230 [a]	10200
8e(up) [d]	0.005	α-methylstyrene (15)	toluene (10)	120	10	1940 [a]	20000
8e(up) [d]	0.003	dimethylitaconate (5)	toluene (5)	140	50	600 [e]	24400
8e(down) [d]	0.005	hexene (15)	toluene (10)	80	10	4870 [a]	6300
8e(down) [d]	0.004	styrene (15)	toluene (10)	80	10	2414 [a]	24100
8e(down) [d]	0.004	cyclohexene (15)	toluene (10)	120	10	600 [a]	6300
8e(down) [d]	0.005	α-methylstyrene (15)	toluene (10)	120	10	1820 [a]	20000
8e(down) [d]	0.003	dimethylitaconate (5)	toluene (5)	140	50	500 [e]	31500

[a] The experiments were conducted with a Büchi press gas flow controller. The TOFs where determined in the first 10 min of the experiments. The products were identified by NMR spectroscopy. [b] The TOF was measured in situ by ATR-IR spectroscopy in the range from 40 to 100 bar and extrapolated to 10 bar. [c] 3 μL MeCN were added to the reaction mixture. [d] 100 μL $HSiEt_3$ were added to the reaction mixture. [e] The reactions were carried out in a closed autoclave system without monitoring during the reaction. Instead, the TOFs were calculated after the pressure did not further decline in the autoclave. The conversion was determined by GC−MS.

dx.doi.org/10.1021/ja107245k |*J. Am. Chem. Soc.* 2011, 133, 8168–8178

the reaction of unsaturated catalytic species with this solvent. For **3d** it was found that the addition of small amounts (5−10 equiv) of MeCN is crucial for proper catalytic performance. However, a too large amount of acetonitrile led also to lower TONs and TOFs, presumably caused by competitive substrate blocking with the acetonitrile ligand. This demonstrated that the activities of the given rhenium catalysts can be quite sensitive to the choice of the reaction medium. However, in contrast to this, catalytic reactions with **8e** were found to be less dependent on the type of solvent. TONs of more than 24000 could be reached for styrene hydrogenations without decrease of activity until the substrate was fully consumed. Despite this quite intriguing result, we had to realize that the **8e(up)** and **8e(down)** catalysts were not as efficient in the hydrogenation of 1-hexene. This, however, could not be explained by missing catalyst stabilities alone. Rather, we observed a concomitant and intervening isomerization reaction transforming 1-hexene into *Z*/*E*-2-hexene, which was found to proceed at a rate comparable to that of hydrogenations under catalytic conditions (80 °C, 10 bar H_2). We assume that the *Z*/*E*-2-hexenes bind less strongly to rhenium, and thus, the substrate stabilization is lowered as soon as all of the 1-hexene substrate is either hydrogenated or isomerized. As a consequence, early decay sets in, since the stabilization of the catalyst by the formation of stable olefin complexes seems no longer possible. The catalytic performance of the two isomers, **8e(up)** and **8e(down)**, in hydrogenations was found to differ, pointing to the fact that under catalytic conditions an **up**−**down** isomerization[13] does not take place. In absolute numbers, however, these differences were small (Table 1). In addition to this, we explored the catalytic potential of **3a**,**b**,**d**, **5c**, and of **8e(up/down)** in the hydrogenation of the sterically more demanding disubstituted substrates cyclohexene, α-methylstyrene, and dimethyl itaconate. **3a**,**b**,**d** and **5c** showed virtually no activity for these substrates, while **8e(up)** and **8e-(down)** were found to be moderatly active (Table 1).

Attempts to identify the nature of the catalyst's remains from the reaction solutions after the hydrogenation experiments with **3a**,**b**,**d**, **5c** and **8e** failed. Moreover, these remains were not active in subsequent hydrogenation experiments. From this observation we conclude that these catalyzes apparently do not constitute "living" systems. This could be explained on the basis of formation of the compounds [ReBrH(MeCN)(NO)(P∩P)] **10a**−**d** described in the next sections, which were found to be unstable. In the case of **8e(up/down)** the hydrogenations of non-styrenic substrates proceeded under generally lower TOFs and TONs. They were limited by a progressive catalyst deactivation. It is presumed that the crucial catalytic species are the $16e^-$ complexes **2a**−**e**, and it is their missing or too weak stability that restricts the TONs. The unsaturated Sixantphos complex **2e** is stabilized via ortho metalation and concomitant H_2 release to form **7e**. This could be substantiated further by deuteration experiments, which revealed that, under catalytic conditions using D_2, the phenyl groups of the Sixantphos ligand of **8e** became deuterated in the ortho positions. The reversibility of the ortho metalation is the basis for its protection function to the unsaturated [ReBrH(NO)(P∩P)] species. The deactivation of the catalysts was found to be substrate and catalyst precursor dependent and followed for the olefinic substrates approximately the order of their metal-binding capabilities: 1-hexene < styrene ≪ cyclohexene, α-methylstyrene, dimethylitaconate.

At this point, summarizing the facts accumulated from the hydrogenation experiments, we propose an Osborn-type cycle proceeding along the catalytic pathway depicted in Scheme 3

Scheme 3. Proposed Osborn-Type Catalytic Cycle for Catalytic Hydrogenations with 3a,b,d, 5c and 8e

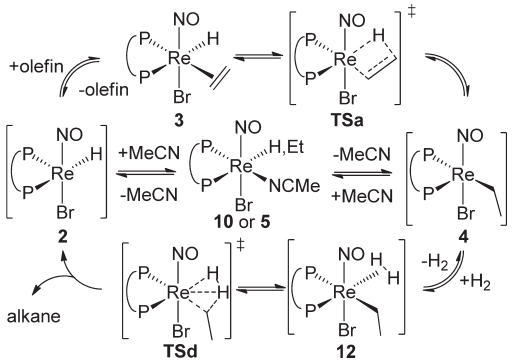

starting from **3a**−**e** as precatalysts. The crucial steps are the formation of the alkyl complexes of type **4** proceeding via the transition state **TSa** and the subsequent hydrogenolysis step of the alkyl−rhenium bonds, which is expected to occur via the dihydrogen complexes of type **12** or/and the dihydride species of type **13** via **TSd** (vide infra DFT calculations). From kinetic measurements we concluded that the overall rate of the hydrogenation is first order in c(cat) and p_{H_2} but zeroth order in c(olefin) and no significant kinetic isotope effect could be determined. These observations would not contradict the proposed cycle but would, on the other hand, also not particularly support it. This made it necessary to devise further detailed mechanistic experiments to acquire more information on unique and separately conducted elementary steps of the catalyzes with **3a**−**e**. The results of these studies are presented in the subsequent sections.

3. MECHANISTIC INVESTIGATIONS OF THE CATALYTIC HYDROGENATION

3.1. Studies on the *β*-Hydride Shift Step. The feasibility of the *β*-hydride shift step as an initial step of the catalytic cycle was indicated by the fact that the equilibrium of eq 1 could be observed. The line shapes of the ^{1}H NMR spectrum of **3c** indicated at room temperature fast Re−H/C_2H_4 proton exchange caused by the reversible *β*-hydride shift reaction connecting **3c** with the unsaturated ethyl complex **4c** (vide infra). Because the line shapes of the ^{1}H NMR spectrum of **3c** were found to be independent of the c(**3c**) and c(MeCN) concentrations, the nonobservable species **4c** connecting **3c** with **5c** is generated from **3c** via an intramolecular reaction (*β*-hydride shift). In order to exclude that this equilibrium is a peculiarity of the **3c**/**5c** system, the MeCN association equilibria were determined quantitatively also for **3a** and **3b** (Table 2).

It was noticed that the *β*-hydride shift reaction causes exchange of the H(Re) and the ethylene protons according to the mechanism depicted in Scheme 4, which became nicely visible in the ^{1}H NMR spectra of compounds **3a**−**d** (500 MHz, 300 K).[14] In Scheme 4 this reversible process was denoted as hydride exchange. It could be observed for all derivatives **3a**−**d** with coalescing signals of the H(Re) moieties and the CH_2 protons in the vicinity to the Re−H group. In the case of **3a**−**c** the H^1/H^2 nuclei display well-defined individual signals. This indicates that **3a**−**c** undergo exclusively the reversible hydride exchange. For **3a** the rate of this exchange could be quantified in a temperature

dx.doi.org/10.1021/ja107245k |*J. Am. Chem. Soc.* 2011, 133, 8168–8178

Table 2. K_d, ΔH, and ΔS of the Equilibrium 5a−c ⇆ 3a−c + MeCN

reaction	K_d (300 K)	ΔH [kJ mol^{-1}]	ΔS [J mol^{-1} K^{-1}]
5a/3a	0.9	18.1	60
5b/3b	29.8	12.5	71
5c/3c	0.04	30.8	74

Scheme 4. Schematic Sketch of the Hydride and the Phosphine Exchange Mechanism

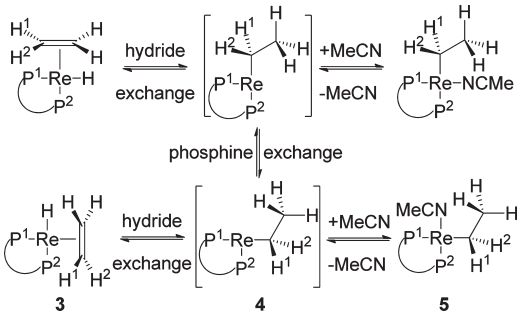

range of 240−300 K in 10 K intervals by means of an NMR simulation, from which the activation parameters ($\Delta H^{\ddagger}$ = 62 kJ mol^{-1} and $\Delta S^{\ddagger}$ = 31 J mol^{-1} K^{-1}) were calculated using transition state theory.[18] In the case of **3b** the signal shapes of the involved protons suggested that the process proceeded with a rate comparable to that of **3a**. In the cases of **3c** and **3d** the exchange proceeded even faster. Quantification of the exchange was in these cases not possible, because unfavorable signal overlaps of the **5c** ⇆ **3c** + MeCN equilibrium or the lack of suitable solvents prevented scrutiny. In addition to the hydride exchange of Scheme 4, the process denoted as phosphine exchange caused coalescing H^1/H^2 and P^1/P^2 resonances, only observed for **3d** at room temperature. In neither case was evidence provided for an exchange involving all of the C_2H_4 protons and the H(Re) atom. This indicated that the C_2H_4 ligand is tightly bound on the NMR time scale and does not undergo free rotation or fast reversible dissociation, since this would be expected to go along with the exchange of all C_2H_4 proton signals. It was concluded from these observations that the β-hydride shift process is the primary elementary step of the given Osborn catalytic cycles.

3.2. Interception of Intermediates of the Catalytic Cycle. Pursuing the hydrogenation of ethylene with **3a**, **3b**, **3d**, and **5c** by NMR spectroscopy revealed that these ethylene or the related ethyl complexes are the only observable reaction intermediates. Further support of the proposed mechanism was envisaged to come from the detection of type **2**, **4**, **12**, and **13** intermediates. In the previous section the dynamics of the β-hydride shift step in **3a**−**d** and of the MeCN complexes **5a**−**c** were analyzed in detail. They were considered as intercepted forms of the [ReBr(Et)(NO)(P∩P)] (**4**) species, and since they are resting states of the catalytic cycles, they could be suitable entries into catalysis. As mentioned before the 16e$^-$ complexes of the form [ReBrH(NO)(P∩P)] (**2**) are assumed to be very unstable and could not be prepared directly from type **1** complexes.[13] Therefore, we attempted studies of the reactions of **3a**, **b**,**d**, **5c**, and **8e** with H_2 in the absence of an olefinic substrate (Scheme 5). This did not, however, allow isolation of type **2** complexes. In the case of **3b** and **8e** the [ReBrH(NO)(P∩P)] fragments were converted to the form of μ^2-H bridged [{ReBrH(NO)(P∩P)}$_2$] dimers **9b** and **9e** obtained as poorly soluble single crystals suitable for structural characterization. In contrast to this **5c** produced the moderatly stable MeCN complex [ReBrH(MeCN)(NO)(dpephos)] (**10c**) instead of the μ^2-H bridged dimer. **10c** was characterized by NMR spectroscopy. As expected the hydride ligand gave rise to a resonance at 1.95 ppm (^2J(H-*trans*-P) = 96.0 Hz, ^2J(H-*cis*-P) = 25.5 Hz) with distinct coupling constants to the cis and the trans phosphorus nuclei. In the ^{31}P NMR spectrum a resonance at 18.1 ppm (^2J(H-*cis*-P) = 25.5 Hz, coupling not fully resolving) and doublet at −5.1 ppm (^2J(H-*trans*-P) = 96.0 Hz) were observed strongly supporting the proposed structure with chemically inequivalent phosphorus nuclei (Scheme 1). Unlike for the reactions of **3b**, **5c**, and **8e** with H_2, the same reactions with **3a** and **3d** led to noncharacterizable, insoluble precipitates. But reaction of **3a**, **3b**, and **3d** with additional amounts of MeCN and H_2 furnished the acetonitrile hydride complexes **10a**, **10b**, and **10d** with spectroscopic features[14] similar to those of **10c**. Since complexes of type **9** and **10** represent also intercepted forms of the highly reactive intermediates of type **2**, which are produced under hydrogenation conditions from type **3** and **5** complexes, it seems plausible that type **2** complexes are intermediates in the catalytic hydrogenation reactions of type **3** and **5** complexes. In contrast to the intermediates of type **2** and **4**, the intermediate H_2 or dihydride complexes **12** or **13** could not be traced spectroscopically, nor could they be intercepted. Thus, structures of type **12** and **13** are presumably located at higher energies getting involved in the rate-limiting part of the catalytic cycle.

Scheme 5. Reaction of Type 3 Compounds with H_2, MeCN and C_2H_4

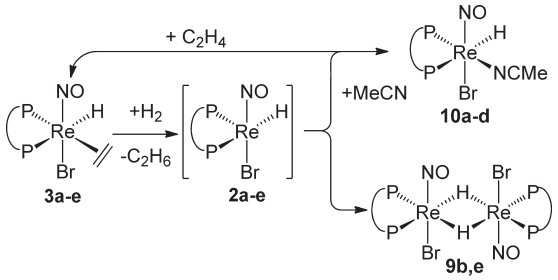

3.3. Isolated Reaction Steps Supporting the Mechanism of the Catalytic Cycle. *3.3.1. Reactions of **3a**−**d** and **5a**−**d** with H_2, MeCN, and C_2H_4.* Characterization of the most abundant reaction intermediates **3a**−**d** and **5a**−**d** and also of the hydride compounds **10a**−**d** allows subdivision of the catalytic cycle into a H_2-splitting reaction and an olefin-binding reaction (Scheme 5). For instance, in NMR experiments the reaction of **3a**−**d** and **5a**−**d** and H_2 led in the presence of MeCN via type **2** intermediates to ethane and **10a**−**d**, which were found to regenerate **3a**−**d** and **5a**−**d** upon exposure to ethylene.

3.3.2. Catalytic Olefin Isomerization Reactions. The courses of Osborn type hydrogenations often are accompanied by olefin isomerization.[1b] Therefore, the catalytic olefin isomerization in some cases side-tracking the olefin hydrogenation catalyis had to be probed. "Ex-situ" catalytic olefin isomerization was attempted with **3a**,**b**,**d** and **5c** with 1-hexene in the absence of H_2. The premises of such experiments were the following:

1. Olefin isomerization would require olefin exchange at the rhenium center and would thus provide a measure for the stability of the Re-olefin complexes. So far we had experienced that olefin exchange is not observable in solutions

dx.doi.org/10.1021/ja107245k |J. Am. Chem. Soc. 2011, 133, 8168–8178

with **3** and **5** complexes in the time frame of the NMR time scale (section 3.1).

2. The binding preferences for certain olefin isomers will become visible. Olefins with favorable binding properties will bind to type **2** complexes and can be isomerized. Olefins with unfavorable binding properties will be exempted from binding to the rhenium centers and could thus not be isomerized. The final product distribution of the olefin isomerization process was expected to show accumulation of the isomer with the least binding affinity unless the thermodynamics of the isomerization process predetermine other preferences.

Exemplarily the isomerization of 1-hexene was investigated. The order in thermodynamic stability of the hexenes is as follows:[27] *E*-3-hexene ($\Delta H^\circ_f = -86.1$ kJ mol^{-1}) < *E*-2-hexene ($\Delta H^\circ_f = -85.5$ kJ mol^{-1}) < *Z*-2-hexene ($\Delta H^\circ_f = -83.9$ kJ mol^{-1}) < *Z*-3-hexene ($\Delta H^\circ_f = -78.9$ kJ mol^{-1}) < 1-hexene ($\Delta H^\circ_f = -74.2$ kJ mol^{-1}). Therefore, *E*-3-hexene would be the product of a thermodynamically driven isomerization process. In NMR experiments applying **3a**−**d** (5 mg) as a catalyst and 1-hexene (50 μL) as a substrate in $CDCl_3$ (500 μL) solutions at 295 K, the following order of activity (TOF/rate of 1-hexene consumption) was observed: **3d** (14 h^{-1}) > **3c** (5 h^{-1}) ≫ **3a,b** (0.3 h^{-1}). The reactions were found to be first order in c([Re]) and zeroth order in c(1-hexene). The initial products were *Z*-2-hexene and *E*-2-hexene in an approximate 1:1 ratio, which could be verified by quantitative ^{13}C NMR spectroscopy.[19] However, exclusively *E*-2-hexene was observed after prolonged reaction times. Isomers of the 3-hexenes were not detectable. Furthermore, the $^{31}P\{^1H\}$ spectra of the reaction solutions revealed signals in addition to those of the catalysts, which were associated with the corresponding hexene complexes. Finally, the ethylene complexes **3a**−**d** were recovered as the only metal-containing products after the removal of the volatiles. This reaction course allowed the following conclusions:

1 Because the thermodynamic product *E*-3-hexene was not found, the product formation should be kinetically determined.
2 Dissociations of the 2-hexenes from **3** proceed with comparable rates. Compared to ethylene both 2-hexene isomers bind weaker to **2a**−**d** otherwise **3a**−**d** could not be recovered as the sole rhenium containing product.
3 Terminal alkenes coordinate stronger than internal ones. Otherwise the isomerization rate would not be zeroth order in c(1-hexene) and the overall reaction rate would also depend on the changing concentrations of the other hexene isomers.
4 The initially formed mixture of *Z*/*E* 2-hexene is eventually isomerized to the thermodynamically more favorable *E*-2-hexene. This indicates that *Z*-2-hexene can still coordinate to Re centers.

In this context the principal question arises whether the observed olefin isomerization rates can be related to the exchange rate of the olefins and to the ethylene dissociation pre-equilibrium. To get further insight into this reaction the activation parameters for the exemplary isomerization reaction of 1-hexene applying **3c** were determined in the temperature range of 295.15−318.15 K (ΔH = 94 kJ mol^{-1}, $\Delta S^{\ddagger}$ = 90 J mol^{-1} K^{-1}). The large $\Delta S^{\ddagger}$ indeed supports the hypothesis that olefin dissociation is rate limiting and that the observed isomerization rates reflect dissociative olefin exchange. However, the nature of the underlying detailed isomerization mechanism is still unclear. Two alternative mechanisms could be envisaged:

1. Isomerization via reversible β-hydride shift reactions in combination with rotation of the β-carbon moiety similar to the process observed for **3a**−**d** (Scheme 7). Such a mechanism was found to be responsible for olefin isomerizations in conjunction with Rh-catalyzed hydrogenations[1b] and hydroformylations[20] of olefins.
2. Isomerization via the formation of an allyl complex. This mechanism would require the generation of an unsaturated intermediate (e.g., dissociation of one phosphorus donor) prior to the formation of an allyl ligand presumably established via oxidative addition of a C−H bond adjacent to the olefinic bond. Such a mechanism was discussed for the olefin isomerization concomitant with Ni-catalyzed hydrocyanation[21a,b] of olefins (along with other mechanisms) or for some Rh- and Ir-catalyzed hydrogenations.[21c]

Scheme 6. Proposed Mechanism for the Observed HD Exchange

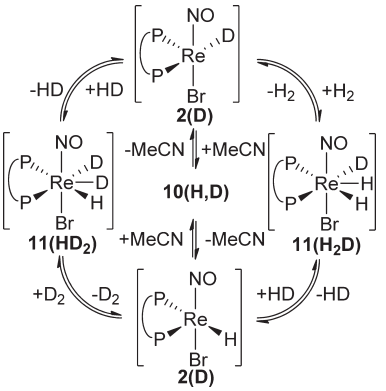

The two mechanisms cannot be distinguished with the available experimental data. However, DFT calculations support mechanism 1 (vide infra). It is noteworthy that the isomerization processes of **3a,b,d** and **5c** catalysts are at 295 K several orders of magnitude slower than the rate of the catalytic hydrogenation. This circumstance supports the assumption of a very strong Re−olefin bond and is in agreement with the zeroth order dependence of c(olefin) on the hydrogenation rate. This is in contrast to rhodium-based Osborn-type hydrogenation catalysts, where the Rh−olefin bonds are weaker and the olefin isomerization and hydrogenation rates were reported to be first order in c(olefin).[1b,c]

3.3.3. H_2/D_2 Isotope Scrambling. Another type of experiment, which was carried out to support the proposed catalytic cycle were H_2/D_2 scrambling reactions. They were thought to provide strong evidence for the existence of type **2** and type **11** complexes. Exposing a mixture of H_2/D_2 to **10a**−**d** results in isotope scrambling within minutes to form HD, which was pursued by ^{1}H NMR spectroscopy. We propose the trihydride complexes $[ReBrH_3(NO)(P\cap P)]$ **11a**−**d** as key intermediates, which are structurally related to the alkyl intermediates of type **13** (Scheme 6).

4. DFT STUDIES ON THE *CIS*-PHOSPHINE $[ReBrH(\eta^2\text{-}C_2H_4)(NO)(PMe_3)_2]$ MODEL SYSTEM

4.1. The Hydrogenation Cycle. The hydrogenolysis step of the Re−alkyl bond in type **4** complexes occurring via type **12** and

dx.doi.org/10.1021/ja107245k |*J. Am. Chem. Soc.* 2011, 133, 8168–8178

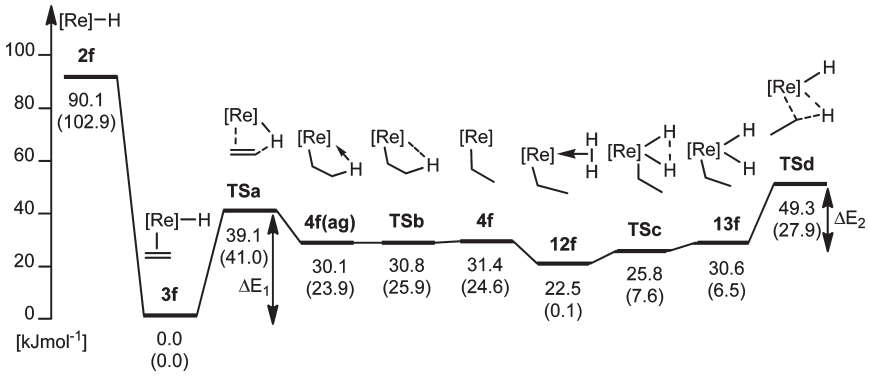

Figure 2. Calculated free energies (and electronic energies in brackets) of the structurally optimized model species along an Osborn-type reaction path.

13 species (Scheme 3) could not be observed spectroscopically. Therefore, we attempted elucidation of this part of the catalytic cycle by DFT calculations using a model system, in which the diphosphines of the Re catalysts were replaced by cis-arranged PMe_3 ligands. The employed PMe_3 model and the methodology[22] (the aptitude of which is discussed in ref 23) are the same as Liu et al. used in their thorough investigation[23] of the hydrogenation catalysis with the *trans*-phosphine $[ReH_2(\eta^2\text{-}C_2H_4)(NO)(PMe_3)_2]$ compound. The PMe_3-substituted structures of types **2**−**4**, **12**, and **13** of the ethylene hydrogenation course of Scheme 3 were denoted as **2f**−**4f(ag)**, **12f**, and **13f** and the related transition states as **TSa** connecting **3f** with **4f(ag)**, **TSb** connecting **4f(ag)** with **4f**, **TSc** connecting **12f** with **13f**, and **TSd** connecting **13f** with **2f**. These structures were optimized without constraints (Figure 3). Their relative energies along the Osborn-type reaction path are shown in Figure 2. The calculations revealed two substantial barriers ΔE_1 (39.1 kJ mol^{-1} β-hydride shift via **TSa**/ethylene insertion) and ΔE_2 (18.8 kJ mol^{-1} reductive elimination of ethane from **13f**). The barrier ΔE_1 corresponds to the β-hydride shift reaction observed in the ^{1}H NMR spectra of **3a**−**d** discussed in section 3.1. For the PMe_3 model system this barrier was found to be lower (39.1 kJ mol^{-1}) compared to the barrier in **3a** (62 kJ mol^{-1}). However, because the exchange in **3a** is the slowest of the **3a**−**d** series and type **3** complexes were found to be quite sensitive to the nature of the employed diphosphine, this is not surprising and it is still in line with the proposed catalytic cycle. Smaller barriers were found for the breakage of the β-agostic Re···H(ethyl) interaction in **4f(ag)** to form **4f** via **TSb** and for the oxidative addition of the H_2 ligand of the H_2 complex **12f** to form the dihydride **13f** via **TSc**. At the level of the free energies of these interconversions at 298.15 K the relative free energies of the involved species change such that **TSb** and **TSc** lose their barrier character due to favorable contributions of E_{rot}, E_{trans}, and E_{vib}. According to the relative energies of the catalytically relevant species, **3f** is the most abundant reaction intermediate (which is also in agreement with the experiment), and **TSd** is the highest energy transition state. The free energy span between these two species is 49.3 kJ mol^{-1}. Employing Shaik's kinetic model[24] for this reaction cycle reveals a TOF control of **3f** and **TSd** of $X_{TOF,I} = 1$ and $X_{TOF,T} = 0.92$, whereas the initial β-hydride shift step and the oxidative addition of H_2 are of minor importance for the TOF.[25] Moreover, the free energy profile in Figure 2 reveals a H_2 binding energy of −8.9 kJ mol^{-1} for **4f**, while the unsaturated complex **2f** displays an ethylene binding energy of −90.1 kJ mol^{-1}. Therefore, the model catalyst would be saturated with the olefin already at lowest concentrations, forming the most abundant reaction intermediate **3f**. Saturation of the system with H_2 would be difficult to achieve, because the H_2 complex **12f** is 22.5 kJ mol^{-1} higher in energy than the most abundant reaction intermediate **3f**. This explains the observed independence of c(olefin) and the linear dependence of c(H_2) of the hydrogenation rate employing **3a**,**b**,**d**, **5c**, and **8e** as catalysts. In the case of **3b** the rate of the 1-hexene hydrogenation was linearly dependent on p_{H_2} up to a pressure of 100 bar.

Comparing the course of the catalytic reaction along the calculated intermediates of the *cis*-$[ReBrH(\eta^2\text{-}C_2H_4)(NO)(PMe_3)_2]$ model catalyst with the course of the *trans*-$[ReH_2(\eta^2\text{-}C_2H_4)(NO)(PMe_3)_2]$ catalyst[23] revealed that both systems follow basically the same Osborn-type mechanism, but in the case of the *cis*-PMe_3 system the involved species are all at lower energies. The energy span between the transition state of the highest energy and the intermediate of the lowest energy is 49.3 kJ mol^{-1} in the *cis*-PMe_3 system compared to 106.3 kJ mol^{-1} (path 1, span between *trans*-$[ReH_2(\eta^2\text{-}C_2H_4)(NO)(PMe_3)_2]$ and oxidative addition of H_2) or 121.3 kJ mol^{-1} (path 2, span between *trans*-$[ReH_2(\eta^2\text{-}C_2H_4)(NO)(PMe_3)_2]$ and reductive elimination of ethane) in the *trans*-PMe_3 system.[23] Furthermore the barrier of the initial β-hydride shift step was found to decline from 87.0 kJ mol^{-1} (*trans*-PMe_3[23]) to 39.1 kJ mol^{-1} (*cis*-PMe_3). Thus, our initial assumption that changing the phosphine arrangement from trans to cis would increase the activity of the catalysts is also reflected in the DFT calculations.

A discussion of the structural changes along the *cis*-PMe_3 catalytic cycle may commence with **3f**, in which the ethylene is bound slightly asymmetric with the Re−C bonds in the typical range of single bonds (C1−Re 2.25 Å, C2−Re 2.29 Å). The C1−C2 bond is considerably stretched to 1.41 Å compared to typical olefinic bonds[27] (1.35 Å) indicating strong back bonding. This is in reasonable agreement with the Re−C bond lengths (2.216(2) and 2.242(3) Å) and the C−C bond length (1.401(4) Å) observed in the structure of **5d**. The geometry of the PMe_3 ligands (Re−P1 2.479 Å, Re−P2 2.541 Å, ∠P1−Re−P2 95.1°) in the model is also in very good agreement with the structure of **5d** (Re−P1 2.4597 (7) Å, Re−P2 2.5691(6) Å, ∠P1−Re−P2 95.22(2)°). The Re−H bond is 1.68 Å, the C1−H(Re) is 2.35 Å and the H−Re−C1 angle is 71.8°. A comparison of the IR spectra of **3a**−**d** with the calculated spectrum (scaled by 0.9614[26]) of **3f** revealed fairly good agreement of the ν(NO) (**3a** 1685 cm^{-1}; **3b** 1678 cm^{-1}; **3c** 1704, 1683 cm^{-1}; **3d** 1673 cm^{-1}; **3f** 1687 cm^{-1}), whereas the ν(ReH) (**3a** 1960 cm^{-1}; **3b** 1974 cm^{-1}; **3c** 2014, 1954 cm^{-1}; **3d** 2009 cm^{-1}; **3f** 1889 cm^{-1}) of the model appears somewhat to much red-shifted. Going from **3f** to **TSa**, the Re−H distance and the H−Re−C1 angle are reduced to 1.51 Å and 40.5°

dx.doi.org/10.1021/ja107245k |*J. Am. Chem. Soc.* 2011, 133, 8168–8178

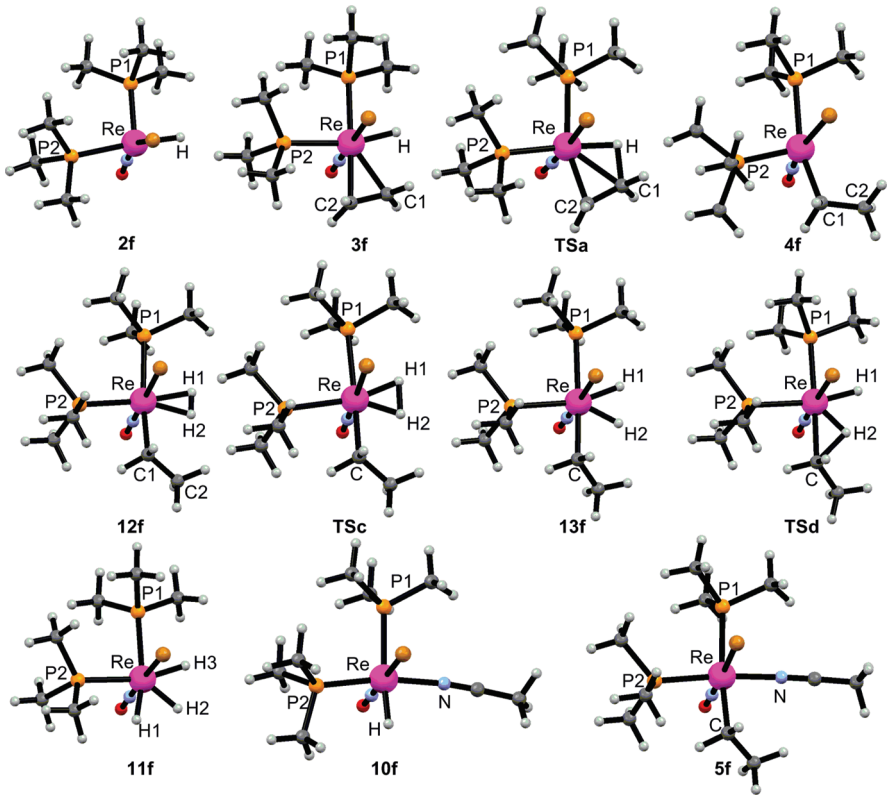

Figure 3. DFT optimized structures of the model compounds **2**−**5f**, **10f**−**13f**, **TSa**, **TSc**, and **TSd**. Selected bond lengths [Å]: **2f** H1−Re 1.69; **3f** C1−C2 1.41, C1−Re 2.25, C2−Re 2.29, H1−Re 1.68, P1−Re 2.54, P2−Re 2.48; **4f** C1−Re 2.18, C1−C2 1.54; **5f** C−Re 2.23, N−Re 2.08; **10f** H1−Re 1.69, N1−Re 2.09; **11f** H1−Re 1.68, H2−Re 1.66, H3−Re 1.68; **12f** C1−Re 2.22, H1−H2 0.84, H1−Re 1.85, H2−Re 1.84; **13f** C1−Re 2.25, H1−H2 1.43, H1−Re 1.68, H2−Re 1.65; **TSa** C1−C2 1.45, C1−H1 1.51, C1−Re 2.32, C2−Re 2.22, H1−Re 1.75; **TSc** C1−Re 2.24, H1−H2 1.24, H1−Re 1.70, H2−Re 1.67; **TSd** C1−Re 2.39, C1−H2 1.63, H1−H2 1.75, H1−Re 1.64, H2−Re 1.68. Selected bond angles [deg]: **2f** P1−Re−P2 103.5; **3f** C1−Re−H1 71.8, P1−Re−P2 95.1; **4f** P1−Re−P2 102.4; **5f** C−Re−N 85.8, C−Re−P2 84.9, N−Re−P1 88.9, P1−Re−P2 99.3; **10f** P1−Re−P2 99.2; **11f**:H1−Re−H2 60.0, H2−Re−H3 60.6, P1−Re−P3 94.7; **12f** C1−Re−H2 74.5, H1−Re−H2 26.4, P1−Re−P2 99.8; **13f** C−Re−H2 64.6, C−Re−P2 79.1, H1−Re−H2 50.9, H1−Re−P1 68.5, P1−Re−P2 95.9; **TSa** C1−Re−C2 37.1, C1−Re−H1 40.5, P1−Re−P2 101.5; **TSc** C−Re−H1 68.8, C−Re−P2 79.9, H1−Re−H2 43.3, H2−Re−P1 70.7, P1−Re−P2 96.3; **TSd** C1−Re−H2 42.9, H2−Re−H1 63.6, P1−Re−P2 95.5.

(significantly below the ca. 2.8 Å of the combined van der Waals radii of C and H[27]). At the same time the Re−H (1.75 Å/+0.06 Å), the Re−C1 (2.32 Å/+0.07 Å) and the C1−C2 (1.45 Å/+0.04 Å) bonds are slightly elongated compared to the respective parameters of **3f**. This suggests that **TSa** retains most of the ethylene hydride character of **3f** and therefore can be called an early transition state. The P−Re−P angle in **TSa** is widened by 6° to 101.5°, favoring in this elementary step the presence of the large-bite-angle diphosphines, since these would perfectly fit **TSa**, but not the starting structure **3f**, and thus are anticipated to promote the β-hydride shift step. This result would explain the large-bite-angle influence of the diphosphines on the real catalytic reaction course, provided that the β-hydride shift step would contribute to the overall barrier height of the catalytic process. From **TSa** the hydride would finally be transferred from the Re atom to the C_2H_4 ligand, resulting in the formation of a 16e$^-$ ethyl species, for which two energetic minima (**4f(ag)** and **4f**) were found. As already mentioned **4f(ag)** is stabilized by a β-agostic interaction between the Me(ethyl) group and the Re center. **4f** was calculated as an unsaturated ethyl complex without agostic interactions. These species are energetically almost equivalent (**4f(ag)** is favored by 1.3 kJ mol^{-1} over **4f** in free energy), and their interconversion via **TSb** is practically barrierless. **4f** possesses a square pyramidal structure with the Et, PMe_3, NO, and the Br ligands in the basal plane and the second PMe_3 ligand in the apical position. The coordination site trans to the apical PMe_3 ligand remains unoccupied and is well accessible. The Re−C1 (2.18 Å) and the C1−C2 (1.54 Å) bonds are both in the typical range of Re−C and C−C single bonds. **4f** then binds H_2 to the vacant coordination site, forming the H_2 complex **12f** with relatively long Re−H distances (1.84 and 1.85 Å) and an elongated H1−H2 distance (0.84 Å). Compared to **4f** the **12f** P−Re−P and the C1−Re−P1 angles are slightly (2.6°; 3.4°) compressed to 99.8° and 91.2°, respectively, reflecting the "steric pressure" originating from the binding of the H_2 molecule. The oxidative addition of the H_2 ligand to form the dihydride complex **13f** proceeds via **TSc**. Compared to those of **12f** the Re−H bonds of **13f** are much shorter (1.68/1.67 Å), and the H−H distance (1.43 Å) is significantly increased and may be denoted as a "compressed" dihydride species.[28] The transition state **TSc** connecting **12f** with **13f** can be characterized as a late transition state, since it is structurally much closer to **13f** than to **12f**, which is reflected in short Re−H bonds (1.70/1.67 Å) and a significantly elongated H1−H2 distance (1.24 Å) still in the range of a "compressed" dihydride structure. Finally, ethane is reductively eliminated from **13f** via **TSd**, which structurally resembles **13f** as a pentagonal bipyramidal structure. Compared to that in **13f** the Re−H1 bond in **TSd** is shortened to 1.63 (−0.04) Å, the Re−C bond is elongated to 2.39 (+0.13) Å, and the C−Re−H1 angle and

dx.doi.org/10.1021/ja107245k |*J. Am. Chem. Soc.* 2011, 133, 8168–8178

Scheme 7. Mechanism of the Olefin Isomerization via the *β*-Hydride Shift Pathway

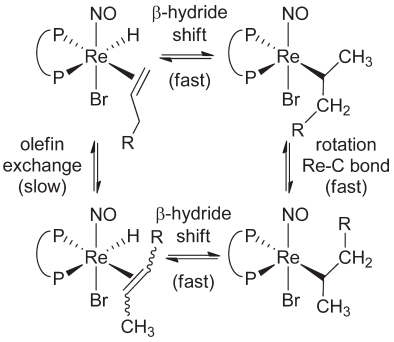

the C−H1 distance are reduced from 64.6° and 2.15 Å in **13f** to 42.9° and 1.63 Å. This can be interpreted as a beginning H transfer to the Re−C bond. At the same time the Re−H2 follows this movement approaching its final position in **2f** trans to the PMe_3 ligand. Upon continuing on the reaction path from **TSd** no further stable intermediate (for instance an agostic structure) could be found, which indicates that **TSd** converts to the product ethane and **2f**, finishing this reductive elimination process or it converts back to **13f**. Overall in these transformations the P−Re−P angle adjusts freely to the Re center's binding needs (**2f** 103.5°, **3f** 95.1°, **4f(ag)** 102.1°, **4f** 102.4°, **12f** 99.8°, **13f** 95.6°, **TSa** 101.5°, **TSb** 102.6°, **TSc** 96.3°, **TSd** 95.5°), while the Br−Re−NO axis remains linear and structurally almost unaffected by any change in the coordinative environment.

4.2. Stabilization of 2f by H_2, MeCN, and C_2H_4 Coordination. The DFT calculations also allowed estimation of the stabilization of **2f** by the addition of H_2 or MeCN. When H_2 is added to the rhenium center, the trihydride **11f** is formed, which results in a stabilization energy of −38.0 kJ mol^{-1} with respect to **2f**. In the case of the MeCN addition forming **10f**, the stabilization energy amounts to −73.6 kJ mol^{-1}. However, for the addition of ethylene transforming **2f** into **3f**, the stabilization energy amounts to −90.1 kJ mol^{-1}, exceeding the stabilization energies from H_2 and MeCN complexations so that on thermodynamic grounds H_2 and MeCN can be displaced by ethylene. The stabilization energy of **2f** from its dimerization to a hypothetical **9f** species was not investigated, since the results were anticipated to be rather artificial and not matching the reality well. It was assumed that the steric congestion of the diphosphines would not be appropriately modeled by PMe_3 ligands. Moreover, the H_2 affinity experiments (section 3.3) provided also evidence that the MeCN complexes of type **10** are thermodynamically favored over the formation of the dinuclear compounds of type **9** (Scheme 5). This further rendered computational model evaluations of the dinuclear structures less significant for the real catalytic reaction course. However formation of **5f** from **4f** by the addition of MeCN seemed to be an appropriate model process to mimic real catalysis and was calculated revealing a ΔE of −26.2 kJ mol^{-1} corresponding to a ΔH of 28.7 kJ mol^{-1} in the gas phase, which would be in the range of the experimentally obtained values for **5a** (ΔH = −18.1 kJ mol^{-1}), **5b** (ΔH = −12.5 kJ mol^{-1}), and **5c** (ΔH = −30.8 kJ mol^{-1}).

4.3. DFT Studies on Olefin Binding in 3f and on the Olefin Isomerization Catalysis. The first three steps in the free energy diagram of Figure 2 can also be envisaged as a part of the olefin isomerization reaction proceeding via a reversible *β*-hydride shift mechanism. In addition to these reaction steps rotation of the alkyl moiety of substituted olefin derivatives of **4f** would be required in order to effect isomerization as sketched in Scheme 7.

Table 3. Olefin Dissociation Free Energies (D_e) of Various Olefin Complexes

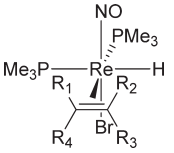

	R_1	R_2	R_3	R_4	D_e(olefin) [kJ mol^{-1}]	d(C−C) [Å]
3f	H	H	H	H	90.1	1.4097
3f$_1$	Me	H	H	H	73.4	1.4140
3f$_2$	H	Me	H	H	77.7	1.4115
3f$_3$	H	H	Me	H	73.2	1.4124
3f$_4$	H	H	H	Me	63.6	1.4140
3f$_5$	Me	Me	H	H	57.3	1.4141
3f$_6$	H	H	Me	Me	44.2	1.4160
3f$_7$	Me	H	Me	H	67.1	1.4151
3f$_8$	H	Me	H	Me	65.1	1.4159

However, since this rotation occurs around a Re−C *σ*-bond, no substantial barriers are expected. Therefore, we expected the olefin complexes of type **3** to be the prevailing reaction intermediates and the unsaturated 16e$^-$ Re-hydride **2f** with the freed olefin to be the highest energy state defining the overall free energy span of the catalytic cycle.

Because the stability of olefin complexes is known to be sensitive to the substitution pattern of the olefin even for alkyl-substituted ones,[29] we calculated all possible propene and 2-butene derivatives of **3f** as PMe_3-substituted model compounds with the intention of explaining the observed selectivity of the isomerization and hydrogenation reactions. The relative stability of these compounds compared to those of **2f** and the free olefins are summarized in Table 3, revealing two important aspects.

1. The inductive effect of the alkyl substituents[29] together with the steric effect of the olefin substitution pattern causes a decline in the relative olefin affinities in the order ethylene > propene > 2-butenes. Although the olefin affinity was found to vary from −44.2 (**3f$_6$**) and −57.3 kJ mol^{-1} (**3f$_5$**) for *Z*-butene to −90.1 kJ mol^{-1} for ethylene, the C−C bond length remained close to 1.41 Å. Thus, it seems that the degree of back-donation is not affected by the variation of the olefin, while the overall olefin affinity varies substantially (Table 3).
2. Steric effects are crucial to olefin binding at rhenium. In particular the large energy difference of 22.9 kJ mol^{-1} between the most favored (**3f$_7$**) and the most disfavored (**3f$_6$**) 2-butene derivatives illustrates that sterics greatly influence also the total energies of the PMe_3 model system. Steric influence can be traced with short distances (below the van der Waals radii) between the Me groups of the olefins and the NO/Br ligands. In the real systems with the more bulky diphosphine ligands, this aspect of the olefin binding might even be more pronounced.

The calculated thermodynamics of the olefin complexes in Table 3 should be interpreted with caution, since the applied "plain" DFT method[22] leads to an incorrect prediction of the thermodynamic stabilities of the butene isomers. The calculated thermodynamic order of the butene isomers is *Z*-2-butene (0.0 kJ mol^{-1}) > *E*-2-butene (+12.8 kJ mol^{-1}) > 1-butene (+12.9 kJ mol^{-1}), whereas the experimental order under standard conditions[27] is

dx.doi.org/10.1021/ja107245k |*J. Am. Chem. Soc.* 2011, 133, 8168–8178

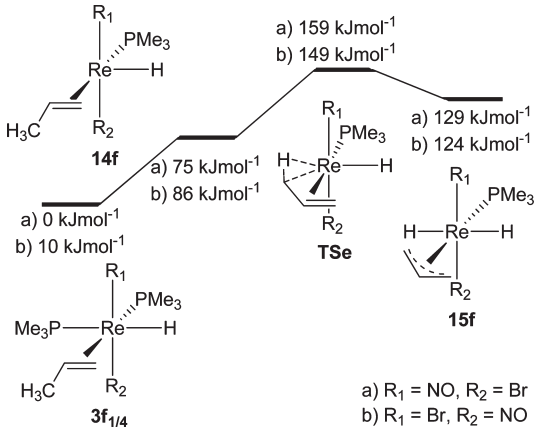

Figure 4. Free energy profile for the isomerization of olefins along the allyl mechanism.

E-2-butene (ΔH^{o}_{f}= −11.4 kJ mol^{-1}) > *Z*-2-butene (ΔH^{o}_{f} = −7.1 kJ mol^{-1}) > 1-butene (ΔH^{o}_{f} = +0.1 kJ mol^{-1}). This is not surprising, since DFT calculations are known to be inaccurate if nonbonding interactions come into play.[30]

To summarize the most important findings we can safely state that the energetic distinction of various isomeric olefin complexes is substantial with a pronounced preference for terminal olefins over internal ones. This also explains the selectivity of the catalysts **3a**,**b**,**d** and **5c** for terminal monosubstituted olefins. The differences in olefin binding arise from electronic and from steric factors. Furthermore, the TOF of the olefin isomerization is determined by the energy span between the most stable olefin complex and the separate 16e^{-} complex **2f** and the corresponding olefin. The reversible β-hydride shift reactions and the rearrangement of the corresponding alkyl complexes of type **4** are anticipated to be much faster and can therefore be considered as a fast pre-equilibrium step.

As an alternative to the isomerization reaction via repetitive reversible β-hydride shift steps, a mechanism proceeding via allyl complexes needs to be considered as well. Therefore, we modeled the unsaturated complex [ReBrH(η^2-propene)(NO)(PMe$_3$)] (**14f**), the allyl complex [ReBrH$_2$(η^3-allyl)(PMe$_3$)] (**15f**), and the transition state **TSe** connecting **14f** with **15f** by means of the same DFT method as applied before. The free energy profile of this sequence is also shown in Figure 4 and revealed a free energy span of 159/148 kJ mol^{-1} between **3f$_{1/4}$** and **TSe**. This is roughly twice as much as for the olefin dissociation, which represents the maximum energy span for the β-hydride shift pathway. Therefore, an isomerization pathway proceeding via the allyl intermediate **15f** can practically be precluded.

5. CONCLUSIONS

This work established that large-bite-angle diphosphine-substituted nitrosyl rhenium complexes of the type [ReBrH(η^2-C$_2$H$_4$)(NO)(P∩P)] are highly active hydrogenation catalysts for olefins, attributing rhenium capabilities hitherto seen only for the series of platinum group metals. An Osborn-type hydrogenation mechanism is proposed, which could be supported by

1. evaluation of the chemoselectivity in the catalytic hydrogenation of substituted olefins,
2. kinetic studies of the catalytic cycle,
3. studies of parts of the catalytic cycle and the interception of intermediates,
4. dynamic NMR analysis of the β-hydride shift step, and
5. accompanying DFT studies.

The basis for this work is the enhanced affinity of appropriately substituted rhenium centers to hydrogen and olefins similar to that of the neighboring group of precious metals. These affinity properties could be exploited for hydrogenation catalyzes only if vacant coordination sites were made temporarily available during the course of the catalytic reaction. Octahedral Re(I) d^6 complexes normally possess high kinetic barriers for such ligand-exchange steps. In the presented systems this problem could be circumvented by appropriately tuned ligand sets enabling a facile β-hydride shift step, which subsequently opens a required vacant coordination site for the oxidative addition of H$_2$. The employed large-bite-angle diphosphines also support Re(I)/Re(III) redox changes favoring the generation of seven-coordinate Re(III) intermediates required in oxidative addition processes. On the basis of the excellent performance of the given, structurally simple rhenium catalysts, we are presently exploring the scope of functional group tolerance in rhenium-based olefin hydrogenation and also enantioselective hydrogenations.

■ ASSOCIATED CONTENT

Supporting Information. Spectroscopic data and experimental procedures for the synthesis of **3a**, **3b**, **3d**, **5c**, **8e(up/down)**, **9b**, **9e**, **10a**, **10b**, **10c**, and **10d**; additional crystallographic data including ORTEP diagrams of **8e(up)**, **8e(down)**, **9b** and **9e**; NMR-simulation data and rates of the **3a**/**4a** exchange process; and equilibrium data for the (**3a**−**c** + MeCN) ⇆ **5a**−**c** equilibrium. This material is available free of charge via the Internet at http://pubs.acs.org.

■ AUTHOR INFORMATION

Corresponding Author
hberke@aci.uzh.ch

■ ACKNOWLEDGMENT

We thank the Swiss National Science Foundation and the University Zürich for financial support.

■ REFERENCES

(1) (a) Osborn, J. A.; Jardine, F. H.; Young, J. F.; Wilkinson, G. *J. Chem. Soc. A* **1966**, *12*, 1711–1732. (b) Schrock, R. R.; Osborn, J. A. *J. Am. Chem. Soc.* **1976**, *98* (8), 2134–2143. (c) Landis, C., R.; Halpern, J. *J. Am. Chem. Soc.* **1987**, *109*, 1746–1754.

(2) (a) Blaser, H. U.; Malan, C.; Pugin, B.; Spindler, F.; Steiner, H.; Studer, M. *Adv. Synth. Catal.* **2003**, *345*, 103–151. (b) Chen, B.; Dingerdissen, U.; Krauter, J. G.; Rotgerink, H.; Mobus, K.; Ostgard, D. J.; Panster, P.; Riermeier, T. H.; Seebald, S.; Tacke, T.; Trauthwein, H. *Appl. Catal., A* **2005**, *280* (1), 17–46.

(3) (a) Zimmermann, S.; Sures, B. *Environ. Sci. Pollut. Res.* **2004**, *11* (3), 194–199. (b) Schmid, M.; Zimmermann, S.; Krug, H. F.; Sures, B. *Environ. Int.* **2007**, *33*, 385–390.

(4) Garrett, C., E.; Prasad, K. *Adv. Synth. Catal.* **2004**, *346*, 889–900.

(5) (a) Heller, D.; Vries, A. H. M.;. de Vries, J. G. In *The Handbook of Homogeneous Hydrogenation*; Elsevier, C. J., Eds.; Wiley-VCH: Weinheim, 2007; pp 1483−1516. (b) Bartholomew, C. H. *Appl. Catal., A* **2001**, *212*, 17–60. (c) Widegren, J. A.; Finke, R. G. *J. Mol. Catal. A: Chem.* **2003**, *198* (1−2), 317–341.

(6) (a) Heinekey, D. M.; Voges, M., H.; Barnhart, D. M. *J. Am. Chem. Soc.* **1996**, *118*, 10792–10802. (b) Bianchini, C.; Marchi, A; Marvelli, L.;

Peruzzini, M.; Romerosa, A.; Rossi, R.; Vacca, A. *Organometallics* **1995**, *14*, 3203–3215. (c) Gusev, D.; Llamazares, A.; Artus, G.; Jacobsen, H.; Berke, H. *Organometallics* **1999**, *18*, 75–89.

(7) (a) Choualeb, A.; Blacque, O.; Schmalle, H. W.; Fox, T.; Hiltebrand, T.; Berke, H. *Eur. J. Inorg. Chem.* **2007**, 5246–5261. (b) Gladysz, J. A.; Boone, B., J. *Angew. Chem., Int. Ed. Engl.* **1997**, *36*, 550–583.

(8) Noyori, R.; Hashiguchi, S. *Acc. Chem. Res.* **1997**, *30*, 97–102.

(9) Kalck, P.; Peres, Y.; Jenck, J. *Adv. Organomet. Chem.* **1991**, *32*, 121–146.

(10) Choualeb, A.; Maccaroni, E.; Blacque, O.; Schmalle, H. W.; Berke, H. *Organometallics* **2008**, *27*, 3474–3481.

(11) Jiang, Y.; Blacque, O.; Fox, T.; Frech, C., M.; Berke, H. *Chem.—Eur. J.* **2009**, *15*, 2121–2128.

(12) Jiang, Y.; Blacque, O.; Fox, T.; Frech, C., M.; Berke, H. *Organometallics* **2009**, *28*, 5493–5504.

(13) Submitted to *Organometallics*

(14) For an in-depth discussion of the spectroscopic features of compounds **3a**−**d**, **5c**, **8e**(**up**), and **8e**(**down**) we refer to the Supporting Information.

(15) Crabtree, R. H.; Gautiér, A.; Giordano, G.; Khan, T. *J. Organomet. Chem.* **1977**, *141*, 113–121.

(16) Landis, C., R.; Brauch, T., W. *Inorg. Chim. Acta* **1998**, *270*, 285–297.

(17) Parkin, G. *J. Labelled Compd. Radiopharm.* **2007**, *50*, 1088–1114.

(18) Eyring, H. *J. Chem. Phys.* **1935**, *3*, 107–115.

(19) Forsyth, D. A.; Hediger, M.; Mahmoud, S. S.; Giessen, B. C. *Anal. Chem.* **1982**, *54*, 1896–1898.

(20) Carvajal, M., .; Kozuch, S.; Shaik, S. *Organometallics* **2009**, *28*, 3656–3665.

(21) (a) Brunkan, N. M.; Brestensky, D. M.; Jones, W. D. *J. Am. Chem. Soc.* **2004**, *126*, 3627–3641. (b) Li, T.; Jones, W. D. *Organometallics* **2011**, *30*, 547–555. (c) Budzelaar, P. M.; Moonen, N. N. P.; de Gelder, R.; Smits, H. M. M.; Gal, A. W. *Eur. J. Inorg. Chem.* **2000**, 753–769.

(22) B3LYP functional, G6-31*+ basis for H-P and Hay and Wadt ECP basis with f polarization functions for Re and Br.

(23) Liu, L.; Bi, S.; Sun, M.; Yuan, X.; Zheng, N.; Li, P. *J. Organomet. Chem.* **2009**, *694*, 3343–3348.

(24) (a) Kozuch, S.; Shaik, S. *J. Am. Chem. Soc.* **2006**, *128*, 3355–3365. (b) Kozuch, S.; Shaik, S. *Acc. Chem. Res.* **2010**, *4*, 101–110.

(25) The TOF control was calculated by employing the program of ref 24a.

(26) Scott, A., P.; Radom, L. *J. Phys. Chem.* **1996**, *100*, 16502–16513.

(27) Lide, D. R. *Handbook of Chemistry and Physics*, 73rd ed.; CRC Press: Boca Raton, FL, 1993.

(28) Kubas, G., J. *Metal Dihydrogen and σ-Bond Complexes*, 1st ed.; Kluwer Academic: New York, 2000.

(29) Tolman, C., A. *J. Am. Chem. Soc.* **1974**, *96*, 2780–2789.

(30) (a) Grimme, S.; Diedrich, C.; Korth, M. *Angew. Chem., Int. Ed.* **2006**, *45*, 625–629. (b) Wodrich, M., D.; Corminboeuf, C.; Schleyer, P. v. R. *Org. Lett.* **2006**, *8*, 3631–3634. (c) Grimme, S. *J. Comput. Chem.* **2006**, *27*, 1787–1799.